Cite this: *Chem. Commun.*, 2011, **47**, 11276–11278

www.rsc.org/chemcomm

COMMUNICATION

Dual colored mesoporous silica nanoparticles with pH activable rhodamine-lactam for ratiometric sensing of lysosomal acidity†

Shuqi Wu,‡[a] Zhu Li,‡[ab] Jiahuai Han[b] and Shoufa Han*[a]

Received 28th July 2011, Accepted 8th September 2011
DOI: 10.1039/c1cc14627k

Alteration of lysosome acidity has been implicated in many biological events ranging from apoptosis to cancer metastasis, *etc*. Mesoporous silica nanoparticles doped with acid activable rhodamine-lactam and fluorescein isothiocyanate (FITC) were developed for ratiometric sensing of lysosomal pH changes in live cells with flow cytometry.

Eukaryotic cells are featured by organelle-specific intracellular pH distribution. For example, the cytosol is nearly neutral (pH 7.2) while the lysosomal lumen is acidic. The acidity of lysosomes is crucial for endocytosis, autophagy, *etc*. Aberrant alterations of the lysosomal pH have been implicated in many pathological events,[1] providing motivation to develop noninvasive and accurate methods for imaging of lysosomal pH. Single intensity based fluorophores are limited in quantitative biological assays due to many uncertainties, *e.g*. local probe concentration. In contrast, ratiometric probes could normalize these interferences, and thus allow accurate quantitation. Many ratiometric pH sensors have been developed utilizing pH sensitive fluorophores along with reference dyes.[2] For example, fluorescein derivatives have been paired with quantum dots, rhodamines, and other dyes to fabricate pH sensors.[2c,i,l,3]

Rhodamine lactams, a group of nonfluorescent compounds hallmarked by intra-molecular lactams, are poised to form highly fluorescent species *via* analyte mediated opening of the lactams.[4] Although rhodamine lactams have been shown to display strong fluorescence in acidic media,[5] their applications in ratiometric pH sensors have not been explored. Mesoporous silica nanoparticles (MSNs) are appealing platforms for bioimaging due to excellent biocompatibility, stability, *etc*.[6] In this report, ratiometric sensing of lysosomal pH in live cells was achieved with dual colored mesoporous silica nanoparticles containing acid activable rhodamine 6G lactam (R6G-lactam) and fluorescein which inversely exhibits decreased fluorescence in acidic media.

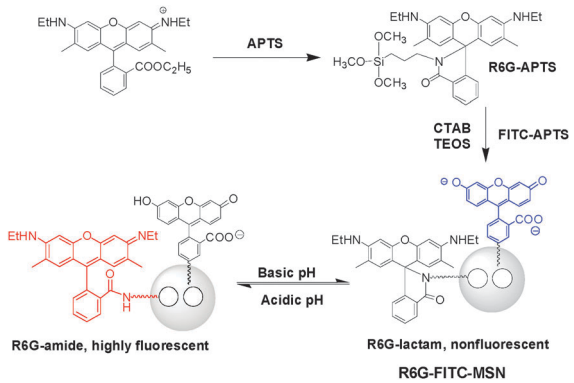

Scheme 1 Preparation of R6G-FITC-MSNs containing two pH sensitive fluorophores.

Aminolysis of rhodamine 6G (R6G) in (3-aminopropyl)-triethoxysilane (APTS) yields nonfluorescent R6G-APTS (Scheme 1). FITC-APTS was synthesized by coupling of the isothiocyanate group of FITC with the amino group of APTS. R6G-APTS and FITC-APTS were then co-condensed with tetraethyl orthosilicate (TEOS) in the presence of cetyltrimethyl-ammonium bromide (CTAB) to give R6G-FITC-MSNs, which were obtained after removal of the unreacted reagents and CTAB.[7] Transmission electron microscopy (TEM) and scanning electron microscopy (SEM) images showed that the dual dye doped MSNs are porous and uniform in size (Fig. 1). Consistently, the average diameter of the MSNs was 110 nm, as determined by dynamic light scattering (ESI†, Fig. S1). R6G-FITC-MSNs were modified with polyethylene glycol to increase the colloidal stability and minimize nonspecific interactions in the subsequent cell assay (ESI†, Scheme S1). Zeta potential analysis of the MSNs showed that the surface potential decreased from 27.9 mV to −6.76 mV after modification, indicating efficient pegylation of the amino groups on the particles (ESI†, Fig S2).

The pH response of R6G-FITC-MSNs was characterized by fluorometry with dual or single wavelength excitation in sodium phosphate buffers of various pH (3.5–7.5). The fluorescence emission peaked at 552 nm increased dramatically as the buffer pH decreased whereas the fluorescein emission centered at 515 nm decreased as the buffer pH lowered (Fig. 2A). The emission, with the spectrum identical to that of rhodamine 6G (ESI†, Fig. S3), was ascribed to the formation of R6G-amide *via* acid mediated opening of R6G-lactam in the nanoparticles (Scheme 1).

[a] *Department of Chemical Biology, College of Chemistry and Chemical Engineering, and the Key Laboratory for Chemical Biology of Fujian Province, Xiamen University, Xiamen, Fujian 361005, China. E-mail: shoufa@xmu.edu.cn; Tel: +86-0592-2181728*
[b] *State Key Laboratory of Cellular Stress Biology and School of Life Sciences, Xiamen University, Xiamen, Fujian 361005, China*

† Electronic supplementary information (ESI) available: Synthesis and characterization of R6G-FITC-MSNs; sensitivity and selectivity of R6G-FITC-MSNs; assay procedures of lysosomal pH in living cells. See DOI: 10.1039/c1cc14627k

‡ These authors contributed equally to this work.

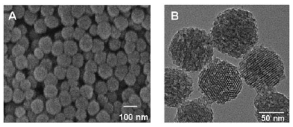

Fig. 1 SEM (A) and TEM (B) images of R6G-FITC-MSNs.

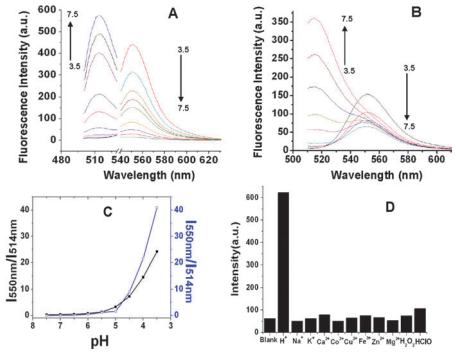

Fig. 2 Characterization of R6G-FITC-MSNs by fluorometry. Fluorescence emission spectra of R6G-FITC-MSN at pH 7.5, 7.0, 6.5, 6.0, 5.5, 5.0, 4.5, 4.0, 3.5 under dual-wavelength excitation (λex@488 nm for FITC and 532 nm for R6G-amide) (A) or single-wavelength excitation (λex@504 nm) (B); (C) pH titration curves of R6G-FITC-MSNs from dual- (in blue) or single-wavelength excitation (in black); (D) selectivity of R6G-FITC-MSN in water for H^+ (λex@532 nm, λem@553 nm).

The R6G-amide in the nanoparticles was 250 fold more bright at pH 4.0 relative to pH 6.5 (Fig. 2A). The titration showed that R6G-lactam, nonfluorescent in cytosolic pH, is sensitive and suitable for lysosome acidity (pH 5.5–3.5) reporting.

The pH dependent fluorescence emissions of R6G-FITC-MSNs under single-wavelength excitation were explored for practical applications. As can be seen from Fig. 2B, emissions of fluorescein and R6G-amide were simultaneously present *via* single-wavelength excitation. As the buffer pH decreased, the emission of R6G-amide increased while that of fluorescein decreased dramatically.

The ratios between fluorescence emission intensity of R6G-amide at 550 nm (I_{550nm}) and intensity of fluorescein at 514 nm (I_{514nm}) were plotted *vs.* pH. The titration curves obtained from either single or dual-wavelength excitation showed that subtle acidification in the range of pH 5.5–3.5 resulted in very large changes in intensity ratio (Fig. 2C). For instance, the I_{550nm}/I_{514nm} interval between pH 4 and pH 5 was 10 for single-wavelength excitation and 20 for dual-wavelength excitation (Fig. 2C). In contrast, previous fluorescein based sensors often exhibited moderate ratio changes (0.3–1) for a fluctuation of one pH unit.[2i,j,l,8] The improved sensitivity could be attributed to the favorable inverse pH responses of R6G-lactam and fluorescein: R6G-lactam exhibited increased fluorescence upon acidification whereas the fluorescence of fluorescein decreased. Overlapping of the lysosome acidity range (pH 5.5–3.5) with the optimal sensing range of R6G-FITC-MSNs (pH 6.0–3.5) suggests its potential applications for monitoring lysosome acidity in cells.

Along with protons, many other ions, *e.g.* K^+ and Mg^{2+}, are ubiquitous in mammalian cells. Some cells could produce chemically reactive species, *e.g.* HOCl and H_2O_2. To be employed as an intracellular pH reporter, it is essential that the R6G-lactam is immune to these interferences. Fluorescein derivatives have been widely used as intracellular pH indicators. Hence the selectivity of R6G-lactam in the MSNs was tested by fluorometry. R6G-lactam sharply responded to H^+ (0.1 mM) and exhibited negligible fluorescence emission in the presence of Na^+, K^+, Ca^{2+}, Mg^{2+}, Zn^{2+}, Cu^{2+}, Fe^{3+}, Co^{2+} (1 mM), H_2O_2 or OCl^- (5 mM) in water (Fig. 2D; ESI†, Fig. S4) or cell culture medium (ESI†, Fig. S5).

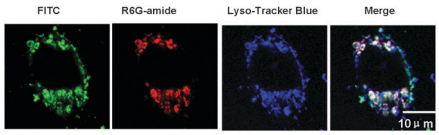

Fig. 3 Intracellular distributions of R6G-FITC-MSNs as compared to LysoTracker Blue DND-22. Bars, 10 μm.

MSNs are readily internalized into cells by endocytosis,[6] leading to accumulation of the particles in lysosomes. To probe the intracellular locations of R6G-FITC-MSNs, L929 cells were co-stained with the nanoparticles and LysoTracker Blue DND-22, which is a lysosome marker from Invitrogen. Microscopic analysis showed that the R6G-amide signal was clearly present in cells (Fig. 3). Colocalization of R6G-amide and DND-22 proved lysosome activated opening of R6G-lactam inside cells. Given the fact that fluorescein fluoresces in extra-lysosomal regions, colocalization of DND-22 with FITC demonstrated that internalized R6G-FITC-MSNs were site-specifically delivered into lysosomes (Fig. 3).

To prove that the fluorescence of R6G-amide was lysosomal acidity dependent, L929 cells were incubated with R6G-FITC-MSNs in the presence or absence of bafilomycin A1 (BFA), which is an ATP–H1 pump inhibitor and is able to alkalinize the lysosomal pH.[9] Microscopic analysis showed that R6G-amide fluorescence colocalized with FITC in cells without addition of BFA. In cells pretreated with BFA where the lysosome acidity was alkalinized, the fluorescence of R6G-amide greatly diminished while FITC signal was still present (Fig. 4), showing that R6G-lactam fluorescence was triggered by the lysosomal acidity, excluding endogenous metal ions induced fluorescence emission inside cells.

To probe the feasibility of ratiometric monitoring of alterations of lysosomal acidity with flow cytometry, L929 cells were pre-cultured with R6G-FITC-MSNs for 2 hours and then incubated in Briton Buffer of various pH containing nigericin, which could homogenize the intracellular pH to that of the incubating buffers.[1c] The cells were analyzed by flow cytometry under single-wavelength excitation. The emissions of R6G-amide (FL2 channel) and FITC (FL1 channel) were readily observed. The plot of FL2/FL1 against pH revealed that pH changes in lysosomes can be conveniently monitored by flow cytometry (ESI†, Fig. S6 and S7).

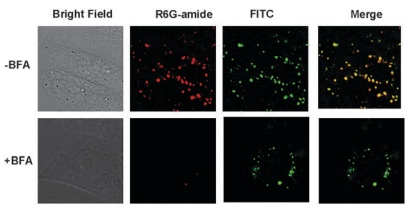

Fig. 4 Confocal microscopic images of fluorescence of R6G-FITC-MSNs in L929 cells treated with or without BFA.

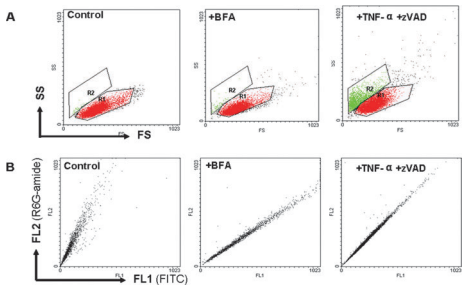

Fig. 5 Monitoring of BFA or TNF-α induced lysosomal pH changes in L929 cells with R6G-FITC-MSNs by flow cytometry. (A) The healthy cells were gated by R1 regions (in red) and analyzed by flow cytometry using single-wavelength excitation (488 nm); (B) fluorescence emission intensity of FITC was recorded by FL1 filter (515–535 nm) while that of R6G-amide was recorded by FL2 filter (560–580 nm).

The lysosomes of U937 cells were alkalinized during apoptosis induced by tumor necrosis factor-α (TNF-α) and zVAD.[10] To explore the utility of R6G-FITC-MSNs in the reporting of lysosomal pH changes, L929 cells were loaded with R6G-FITC-MSNs and then cultured, respectively, with no addition, BFA, or both TNF-α and zVAD. The healthy cells of the three samples were gated and analyzed by flow cytometry under identical settings (R1 region, Fig. 5A). Albeit the amount of the nanoparticles internalized into individual cells varied significantly as indicated by the intensity of R6G-amide or fluorescein, the ratios of FL2/FL1 (slopes) were remarkably constant for the gated populations in each sample (Fig. 5B). The FL2/FL1 values (slopes) were used as the indicators of lysosomal acidity of the samples. The relative lysosome acidity of the samples can be easily differentiated by the corresponding slopes of the samples as shown in Fig. 5B, conforming to the established effects of BFA on lysosomal acidity.[9] Relative to the control, the lysosomes of L929 cells were alkalinized by TNF-α/zVAD, which was consistent with the reported effects of TNF-α/zVAD on U937 cells.[10]

FITC-conjugated dextran, widely used to measure lysosomal pH *via* dual-wavelength excitation,[10,11] suffers from limitations, *e.g.* low sensitivity.[12] Polystyrene particles with Oregon Green 488 were later developed for sensing lysosomal pH in murine macrophages.[12] Different from prior sensors which rely on fluorescein as the pH reporting dye and exhibit decreased fluorescence in acidic conditions, mesoporous silica nanoparticles doped with rhodamine-lactam (acid activable pH reporting dye) and fluorescein (reference dye) were designed for ratio imaging of lysosomal acidity. The favorable inverse responses of rhodamine-lactam and fluorescein in acidic media result in ratiometric lysosome pH determination with high sensitivity.

In summary, mesoporous silica nanoparticles containing lysosome activable rhodamine-lactam were prepared for ratiometric sensing of lysosomal pH changes in living cells with high sensitivity by confocal microscopy or flow cytometry *via* single-wavelength excitation. Alteration of lysosomal pH was involved in several cell signaling pathways.[1b,13] Activation of fluorogenic immuno-conjugates by intra-lysosomal acidity has been used for imaging of viable cancer cells in mice.[14] The features of lysosome activable rhodamine-lactam based nanosensors suggest their potential utility for studies of lysosome-involved cell biology or evaluation of lysosome-targeted cancer therapy.

Dr S. Han was supported by NSF China 20802060, 21072162 and the Fundamental Research Funds for the Central Universities 2011121020; Dr J. Han was supported by NSF China 30830092, 30921005, 91029304, 81061160512 and 973 program 2009CB522200.

Notes and references

1 (*a*) A. Di, M. E. Brown, L. V. Deriy, C. Li, F. L. Szeto, Y. Chen, P. Huang, J. Tong, A. P. Naren, V. Bindokas, H. C. Palfrey and D. J. Nelson, *Nat. Cell Biol.*, 2006, **8**, 933–944; (*b*) E. S. Trombetta, M. Ebersold, W. Garrett, M. Pypaert and I. Mellman, *Science*, 2003, **299**, 1400–1403; (*c*) C. Nilsson, K. Kagedal, U. Johansson and K. Ollinger, *Methods Cell Sci.*, 2003, **25**, 185–194.
2 (*a*) S. Charier, O. Ruel, J. B. Baudin, D. Alcor, J. F. Allemand, A. Meglio and L. Jullien, *Angew. Chem., Int. Ed.*, 2004, **43**, 4785–4788; (*b*) T. Doussineau, M. Smaihi and G. J. Mohr, *Adv. Funct. Mater.*, 2009, **19**, 117–122; (*c*) T. Doussineau, S. Trupp and G. J. Mohr, *J. Colloid Interface Sci.*, 2009, **339**, 266–270; (*d*) J. Han, A. Loudet, R. Barhoumi, R. C. Burghardt and K. Burgess, *J. Am. Chem. Soc.*, 2009, **131**, 1642–1643; (*e*) S. W. Hong, K. H. Kim, J. Huh, C. Ahn and W. H. Jo, *Chem. Mater.*, 2005, **17**, 6213–6215; (*f*) T. Jin, A. Sasaki, M. Kinjo and J. Miyazaki, *Chem. Commun.*, 2010, **46**, 2408–2410; (*g*) J. Lei, L. Wang and J. Zhang, *Chem. Commun.*, 2010, **46**, 8445–8447; (*h*) H. Sun, A. M. Scharff-Pousen, H. Gu and K. Almdal, *Chem. Mater.*, 2006, **18**, 3381–3384; (*i*) T. Jin, A. Sasaki, M. Kinjo and J. Miyazaki, *Chem. Commun.*, 2010, **46**, 2408–2410; (*j*) P. T. Snee, R. C. Somers, G. Nair, J. P. Zimmer, M. G. Bawendi and D. G. Nocera, *J. Am. Chem. Soc.*, 2006, **128**, 13320–13321; (*k*) C. G. Niu, X. Q. Gui, G. M. Zeng and X. Z. Yuan, *Analyst*, 2005, **130**, 1551–1556; (*l*) J. Lei, L. Wang and J. Zhang, *Chem. Commun.*, 2010, **46**, 8445–8447.
3 (*a*) Y. H. Chan, C. Wu, F. Ye, Y. Jin, P. B. Smith and D. T. Chiu, *Anal. Chem.*, 2011, **83**, 1448–1455; (*b*) V. M. Chauhan, G. R. Burnett and J. W. Aylott, *Analyst*, 2011, **136**, 1799–1801; (*c*) H. A. Clark, R. Kopelman, R. Tjalkens and M. A. Philbert, *Anal. Chem.*, 1999, **71**, 4837–4843; (*d*) T. Doussineau, M. Smaihi and G. J. Mohr, *Adv. Funct. Mater.*, 2009, **19**, 117–122; (*e*) S. W. Hong, K. H. Kim, J. Huh, C. Ahn and W. H. Jo, *Chem. Mater.*, 2005, **17**, 6213–6215; (*f*) H. Sun, A. M. Scharff-Pousen, H. Gu and K. Almdal, *Chem. Mater.*, 2006, **18**, 3381–3384.
4 H. N. Kim, M. H. Lee, H. J. Kim, J. S. Kim and J. Yoon, *Chem. Soc. Rev.*, 2008, **37**, 1465–1472.
5 (*a*) T. Hasegawa, Y. Kondo, Y. Koizumi, T. Sugiyama, A. Takeda, S. Ito and F. Hamada, *Bioorg. Med. Chem.*, 2009, **17**, 6015–6019; (*b*) W. Zhang, B. Tang, X. Liu, Y. Liu, K. Xu, J. Ma, L. Tong and G. Yang, *Analyst*, 2009, **134**, 367–371; (*c*) Z. Li, S. Wu, J. Han and S. Han, *Analyst*, 2011, **136**, 3698–3706.
6 (*a*) J. Lu, M. Liong, Z. Li, J. I. Zink and F. Tamanoi, *Small*, 2010, **6**, 1794–1805; (*b*) J. L. Vivero-Escoto, I. I. Slowing, B. G. Trewyn and V. S. Lin, *Small*, 2010, **6**, 1952–1967.
7 Y. Zhao, B. G. Trewyn, I. I. Slowing and V. S. Lin, *J. Am. Chem. Soc.*, 2009, **131**, 8398–8400.
8 H. S. Peng, J. A. Stolwijk, L. N. Sun, J. Wegener and O. S. Wolfbeis, *Angew. Chem., Int. Ed.*, 2010, **49**, 4246–4249.
9 T. Yoshimori, A. Yamamoto, Y. Moriyama, M. Futai and Y. Tashiro, *J. Biol. Chem.*, 1991, **266**, 17707–17712.
10 C. Nilsson, U. Johansson, A. C. Johansson, K. Kagedal and K. Ollinger, *Apoptosis*, 2006, **11**, 1149–1159.
11 S. Ohkuma and B. Poole, *Proc. Natl. Acad. Sci. U. S. A.*, 1978, **75**, 3327–3331.
12 J. Ji, N. Rosenzweig, C. Griffin and Z. Rosenzweig, *Anal. Chem.*, 2000, **72**, 3497–3503.
13 R. W. Van Dyke, *Subcell. Biochem.*, 1996, **27**, 331–360.
14 Y. Urano, D. Asanuma, Y. Hama, Y. Koyama, T. Barrett, M. Kamiya, T. Nagano, T. Watanabe, A. Hasegawa, P. L. Choyke and H. Kobayashi, *Nat. Med.*, 2009, **15**, 104–109.